

Controlled assembly of gold nanoparticles on carbon surfaces

Alison J. Downard,* Emelyn S. Q. Tan and Samuel S. C. Yu

Received (in Durham, UK) 11th April 2006, Accepted 20th July 2006

First published as an Advance Article on the web 9th August 2006

DOI: 10.1039/b605219c

Citrate-capped gold nanoparticles are electrostatically assembled on amine films attached to carbon surfaces. Primary amines are covalently grafted to carbon surfaces by an electrochemically-assisted method which gives easy control of the number of amine functionalities on the surface, and hence the density of the nanoparticle assembly. Further control of nanoparticle assemblies can be gained by choice of the amine modifier, and by adjusting the nanoparticle concentration, assembly time and pH of the nanoparticle solution. This simple and versatile approach for preparation of tethered nanoparticle assemblies should be compatible with any conducting carbon substrate, giving new materials for applications ranging from catalysis to sensing.

1 Introduction

The immobilization of metal nanoparticles on solid surfaces using molecular layers or tethers generates new materials with interesting properties. Diverse applications have been proposed for nanoparticle assemblies, ranging from bio- and chemical sensors to catalysis and nanoelectronics.¹ A range of strategies based on electrostatic interactions,^{2–10} biomolecular recognition^{11–13} and covalent coupling^{2,14–18} have been exploited to tether metal nanoparticles to silicon, glass, metal and plastic surfaces. In comparison to these substrates, carbon has received little attention. Carbon has a unique set of characteristics which makes it an interesting material for assembly of nanoparticles. It can be highly conducting and low cost, and is available in a variety of forms suitable for different applications. For example, screen-printed graphite electrodes can form the basis of disposable bio- and chemical sensors, high surface area carbon powders, felts and cloths form catalyst-supports, fuel cell components and industrial-scale electrodes, and pyrolysed photoresist films (PPFs) and carbon nanotubes are of interest for molecular electronics.

The electrochemically-assisted covalent modification of carbon materials involves the generation of solution-based radical species at the surface, and the subsequent coupling of these radicals with surface atoms.¹⁹ All conducting carbon materials appear to undergo the grafting reaction¹⁹ and there are no limitations with respect to the form of the material (planar surface, powder, cloth, fibres and so on). Oxidation of primary amines^{20,21} to give surface films attached *via* C–N bonds is the focus of this work. At appropriate solution pH, amine moieties are protonated and are expected to assemble citrate-capped gold nanoparticles *via* electrostatic interactions. A similar approach has been demonstrated for the formation of gold nanoparticle assemblies on silicon and gold surfaces,

modified with silanes and alkanethiols, respectively.^{2,3,5–8,10} An advantage of the electrochemically-assisted grafting procedure used in this work is the formation of a covalent bond between the surface and the amine tether, giving an easily prepared, controllable and stable tether film.¹⁹

There has been one report of attachment of gold nanoparticles to planar carbon substrates *via* surface-bound molecular films. Porter and co-workers reported formation of mercaptobenzene films on glassy carbon electrodes by electroreduction of the corresponding diazonium salt, and subsequent assembly of 30 nm gold nanoparticles.²² In a related example, the attachment of gold nanoparticles to thiol functionalized carbon nanotubes was achieved after the direct, solvent-free thermal grafting of the thiol to the nanotube.²³

In this work we demonstrate the attachment of molecular layers to pyrolysed photoresist film (PPF) surfaces *via* the electrochemical oxidation of mono- and diamines, and investigate the electrostatic assembly of citrate-capped Au nanoparticles on amine-modified PPF. Use of planar carbon films as the substrate allows for easy quantification of the nanoparticle assemblies, however the methods can be extended to other forms of conducting carbon.

2 Experimental

Materials

Surface modifiers *n*-hexylamine (NH₂(CH₂)₅CH₃, HA) (Sigma) and tetraethylene glycol diamine (NH₂CH₂CH₂(OCH₂CH₂)₃NH₂, TGD) (Molecular Biosciences) were used as received. 4-methylbenzene (4-MB) diazonium tetrafluoroborate was synthesised using literature methods.²⁴ Acetonitrile (HPLC grade, Ajax Finechem) was dried over CaH₂ for 7 days, and refluxed under N₂ for 120 min prior to distilling in an N₂ atmosphere. Tetrabutylammonium tetrafluoroborate ([Bu₄N]BF₄) was prepared from tetrabutylammonium hydroxide (Acros Organics) and fluoroboric acid (BDH), dried under reduced pressure at 80 °C for 2 days and stored under vacuum. Ferrocene monocarboxylic acid (FCA, Sigma) was used as received. Phosphate buffer (0.04 M, pH 7.4) with

MacDiarmid Institute of Advanced Materials and Nanotechnology, Department of Chemistry, University of Canterbury, Private Bag 4800, Christchurch, New Zealand. E-mail: alison.downard@canterbury.ac.nz; Fax: 64 3 3642110; Tel: 64 3 3642501

added 0.1 M NaCl was used for aqueous electrochemical measurements. Milli-Q water, $>18\text{ M}\Omega\text{ cm}$, was used to prepare aqueous solutions. All electrochemical cells and glassware were dried and stored at $45\text{ }^{\circ}\text{C}$.

Citrate-capped Au nanoparticles were prepared by the method of Natan and co-workers.² The as-prepared solution of colloidal particles was characterised by an absorption maximum at 520 nm. Transmission electron microscopy (TEM) images were obtained using a JEOL 1200EX electron microscope operating at 80 keV. Samples for TEM were prepared by deposition of one drop of nanoparticle solution onto standard Formvar-coated copper grids and drying in air. TEM showed a range of particle diameters from 10–16 nm, with an average diameter of 11 nm. The nanoparticle concentration was calculated assuming all Au was reduced to form particles of diameter 11 nm, giving approximately 1.3×10^{16} nanoparticles L^{-1} .

PPF was prepared as described elsewhere.²⁵ After pyrolysis and cooling to room temperature, the samples were briefly sonicated (3 s) in successive baths of acetone, methanol and isopropyl alcohol, dried with N_2 and stored under vacuum. The typical RMS surface roughness determined from AFM imaging of the surfaces was between 0.2 and 0.5 nm.

Electrochemistry

All electrochemical measurements were performed using a computer controlled EG & G PAR Model 173 potentiostat coupled to a Powerlab 4SP (ADInstruments). Samples of PPF (15 mm \times 15 mm) were mounted horizontally on an insulated metal stage under a glass cell held down by four springs. A Viton O-ring sealed the solution above the PPF giving an electrode area of 0.24 cm^2 . Electrical contact was made using a copper strip placed on the PPF surface not exposed to solution. The auxiliary electrode was a Pt wire and reference electrodes were a saturated calomel electrode (SCE) for aqueous solutions and a Ag/Ag^+ (10^{-2} M AgNO_3 in acetonitrile–0.1 M $[\text{Bu}_4\text{N}]\text{BF}_4$) electrode for non-aqueous solutions. The ferrocenium/ferrocene (Fc^+/Fc) couple appeared at $E_{1/2} = 0.01\text{ V}$ versus Ag/Ag^+ . All electrochemical measurements were made at room temperature in an N_2 atmosphere. Cyclic voltammograms were obtained using scan rate = 100 mV s^{-1} .

Modification of PPF and assembly of Au nanoparticles

Electrochemical grafting of amine and methylphenyl (MP) films to PPF was carried out in 0.1 M $[\text{Bu}_4\text{N}]\text{BF}_4$ -acetonitrile solutions containing approximately 5 mM TGD, HA or 4-MB diazonium salt. A fresh sample of PPF was used for every modification. The standard modification procedure entailed an initial cyclic scan from 0 V to E_{app} at 100 mV s^{-1} , followed by a potential step from 0 V to E_{app} for 10 min. E_{app} was 1.2, 1.3 and -1.12 V for TGD, HA and 4-MB diazonium cation, respectively. A final scan was recorded in the modification solution using the same conditions as for the initial scan. Modified PPF samples were rinsed successively with acetonitrile and water, and dried with compressed N_2 prior to further use, or storage under vacuum.

To obtain static water contact angles for TGD and HA films, the modified PPF sample was placed on a horizontal

stage and 1 μL of Milli-Q water was dispensed onto the surface from a microsyringe. The water droplet image was captured by an Edmund Scientific video camera and Video for Windows NT software. Three measurements were taken from each side of the drop and two drops were applied, sequentially, to each modified surface. The average water contact angle of two separate samples (*i.e.* of 24 measurements) was calculated and the stated errors indicate the range of values obtained.

For assembly of Au nanoparticles, the nanoparticle solution was used as-prepared (pH 4.2), or after diluting with Milli-Q water or adjusting the pH to 7, 8 or 12 by addition of a concentrated NaOH solution. PPF samples were immersed in the solution for the selected time at room temperature. For experiments investigating the influence of immersion time, all measurements were made using the same modified surface (*i.e.* samples were immersed in the nanoparticle solution for 1 min, removed and imaged using SEM, re-immersed in the solution for 21 min, removed and imaged and so on). All other experiments were undertaken using a freshly grafted surface. After treatment, the samples were rinsed with water, dried with a gentle stream of N_2 and stored under vacuum.

Scanning electron microscopy (SEM) images of nanoparticle assemblies were obtained using a Raith 150 e-beam lithography system operating with a 10 keV accelerating voltage. Quantification of nanoparticle assemblies utilised Image Pro Plus software. Four areas of interest $100\text{ nm} \times 100\text{ nm}$ were defined on a $200\,000\times$ SEM image and the nanoparticles counted using the manual tag function. At least two SEM images were obtained for each sample and the average of all nanoparticle counts (at least eight) was calculated for one sample. The values reported are the average of nanoparticle counts for all samples prepared using the same conditions, and the uncertainties indicate the full range of values obtained for all nanoparticle counts.

3 Results and discussion

Covalent attachment of amines to PPF surfaces and electrochemical characterisation

The oxidation of primary amines in anhydrous conditions at glassy carbon (GC),^{21,26–31} carbon felt^{32–34} and carbon fibre^{20,35–37} electrodes has been shown to result in the formation of surface attached films. For this work, we have used PPF, a very smooth carbon material with GC-like properties.^{38,39} Although PPF electrodes usually exhibit very similar electrochemical behaviour to GC,³⁹ in earlier work examining the electrografting of arylacetates, we found an example where markedly different results were obtained at the two surfaces.⁴⁰ Hence in initial experiments we examined the grafting of amines to PPF surfaces, following similar electrochemical procedures to those used at other carbon surfaces. Two amines with different properties were chosen in order to investigate the nanoparticle assembly process. TGD is a diamine and relatively hydrophilic whereas HA is a monoamine and relatively hydrophobic (Chart 1).

Fig. 1A shows a cyclic voltammogram of approximately 5 mM TGD in acetonitrile–0.1 M $[\text{Bu}_4\text{N}]\text{BF}_4$ at a PPF surface, and a second scan recorded in the same solution after the

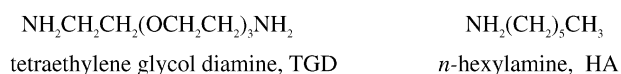
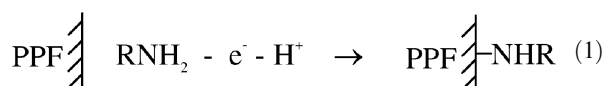


Chart 1

electrode potential had been held at 1.2 V for 10 min. In the initial scan the broad peak at $E_{\text{pa}} \approx 1$ V is assigned to amine oxidation. After 10 min electrolysis, no peak is seen in the voltammograms and the measured current is very low. These results are typical of those observed using other carbon substrates, suggesting that amine oxidation at PPF leads to grafting of a film that alters the surface properties. Prior to modification, the static water contact angle on the PPF surface is $72 \pm 4^\circ$, decreasing to $46 \pm 3^\circ$ after modification, consistent with the formation of a hydrophilic surface film. Eqn (1) shows the proposed electrochemically-assisted coupling reaction.^{20,21}



The voltammetry of the probe redox species, 0.5 mM ferrocenemonocarboxylic acid (FCA), in phosphate buffer with 0.1 M NaCl (pH 7.4) was examined at the PPF surface, before and after the modification procedure. Fig. 1B shows that at a pristine PPF surface, the voltammogram of FCA is chemically reversible with $E_{1/2} = 0.26$ V and $\Delta E_p = 80$ mV. At the TGD-modified surface, the FCA anodic peak potential has shifted more positive, the peak current is lower and there is

no associated reduction peak. These changes are consistent with the presence of a surface film which changes the apparent electron transfer kinetics to the solution species. When the modification conditions are applied to a pristine PPF surface but in the absence of TGD, the voltammogram of FCA at the treated surface is indistinguishable from that obtained before treatment (not shown). Thus the voltammetric response of FCA supports the formation of a surface-attached film by oxidative electrolysis in the presence of amine.

Similar experiments were carried out with HA as the modifier with qualitatively similar results (Fig. 1C, 1D). For modification of PPF, the electrolysis potential was 1.3 V and the resulting film appeared to have greater impact on FCA voltammetry (Fig. 1D) than the TGD film. A film of HA has a static water contact angle of $77 \pm 2^\circ$ and hence is a significantly more hydrophobic surface than TGD. This may account, in part, for the different electrochemical response of FCA.

The shapes of the FCA voltammograms at the modified surfaces (Fig. 1B, 1D) are consistent with the formation of surface films containing amines which can be protonated, to some extent, at pH 7.4. At this pH, the carboxylic acid substituent of FCA will be deprotonated leading to electrostatic accumulation of anionic FCA at the cationic surface film. After oxidation to ferrocenium, FCA has a net zero charge and the electrostatically accumulated FCA diffuses from the interfacial region giving the observed lower currents for reduction than oxidation.

Assembly of Au nanoparticles on amine-modified surfaces

Using standard methods, citrate-capped gold nanoparticles were synthesised with an average particle diameter of 11 nm, a solution concentration of approximately 1.3×10^{16} nanoparticles L^{-1} and pH of 4.2. In initial experiments, TGD- and HA-modified PPF samples, electrografted as described above, were immersed in as-prepared Au nanoparticle solution for 3 h followed by rinsing and drying. Two control samples were also prepared. A modified surface that contains no amine functionalities was generated by electrografting a methylphenyl (MP) film to PPF *via* reduction of the corresponding diazonium cation. A PPF blank was prepared by subjecting a PPF sample to the same modification procedure as for preparation of an HA film, but in the absence of HA. The control samples were treated with Au nanoparticle solution as described above. Fig. 2A–D show typical SEM images of the four types of surface, and all data concerning nanoparticle assemblies are given in Table 1. For the TGD modified surface (Table entry 1, Fig. 2A), a dense coating of Au nanoparticles is assembled (36 ± 8) nanoparticles/ 10^4 nm^2) which gives a clearly visible gold coloration to the surface. On the HA film, the nanoparticle density is approximately 70% less (Table entry 14 and Fig. 2B) and this surface appears green to the eye. Only a few particles adhere to the control surfaces (Table entries 15, 16 and Fig. 2C,D) demonstrating firstly, that assembly on neutral hydrocarbon films is not favourable and secondly that assembly is not promoted on a bare PPF surface that has been treated in the same manner as a film-coated electrode, but in the absence of modifier.

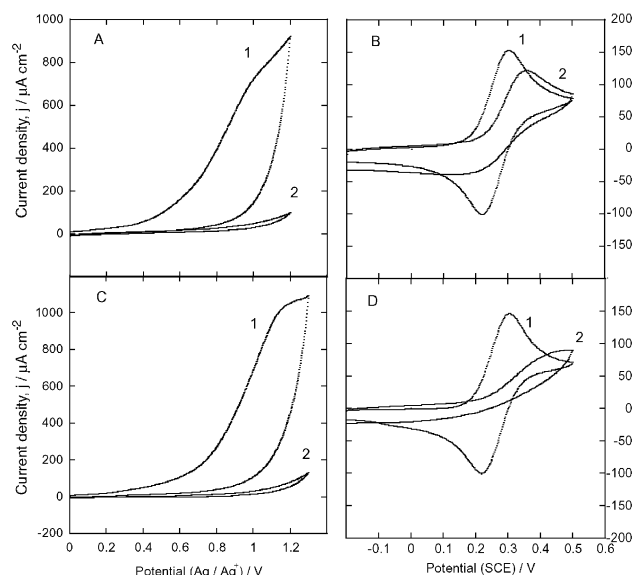


Fig. 1 (A), (C) Cyclic voltammograms, obtained at PPF surfaces, of approximately 5 mM (A) TGD and (C) HA in acetonitrile–0.1 M $[\text{Bu}_4\text{N}]\text{BF}_4$. (1) First scan and (2) scan after holding potential at E_{app} for 10 min. (B), (D) Cyclic voltammograms of 0.5 mM FCA in phosphate buffer with 0.1 M NaCl (pH 7.4), (1) before electrode modification and (2) after electrode modification with (B) TGD and (D) HA. All voltammograms were obtained using scan rate = 100 mV s^{-1} .

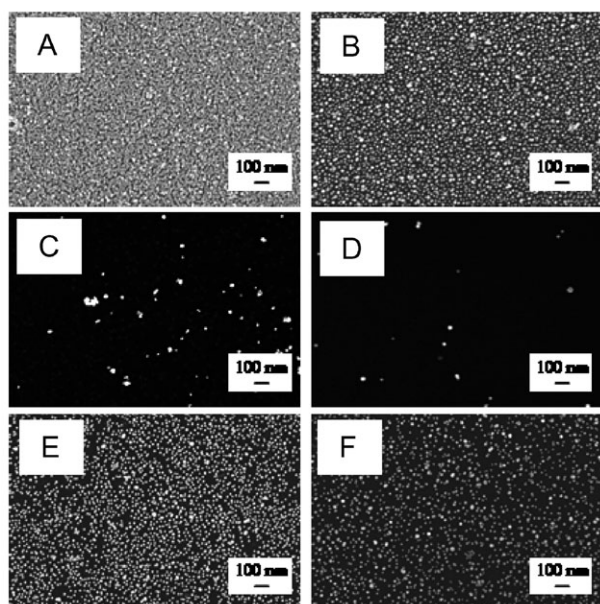


Fig. 2 SEM images of PPF samples treated with nanoparticle solutions (1.3×10^{16} nanoparticles L^{-1} , immersion time = 180 min, pH 4.2 unless noted otherwise). Films were prepared with 600 s electrolysis, except when stated otherwise. (A) TGD film, pH 4.2; (B) HA film, pH 4.2; (C) MP film, pH 4.2; (D) blank, pH 4.2; (E) TGD film prepared with 120 s electrolysis time, pH 4.2 and (F) TGD film, pH 8.

The assembly of nanoparticles on the TGD and HA films at pH 4.2 is controlled by the electrostatic attraction between protonated amines in the films and the negative charge of the nanoparticle citrate capping groups. Several factors can be considered to account for the significantly greater nanoparticle density on the TGD film. First is the number of cationic sites in each film. Although the structure of the films is unknown, simply on the basis that TGD is a diamine and HA a

monoamine, the number of cationic sites incorporated in the TGD film is likely to be greater than in the HA films. This conclusion is based on the assumption that a similar mechanism for formation, and a similar structure, is established for each film. A second factor governing the nanoparticle assembly is the nature of each surface film. Contact angles reveal that for the HA film ($\theta = 77 \pm 2^\circ$), the cationic sites are incorporated in a hydrophobic environment whereas for TGD, the film environment is hydrophilic ($\theta = 46 \pm 3^\circ$). Approach of the hydrophilic citrate-capped nanoparticle to the hydrophobic HA surface may be restricted by the interfacial water to a larger extent than in the case of the TGD film. Similar effects are well-documented in the case of small molecules undergoing electron transfer at alkanethiol monolayers terminated with hydrophobic and hydrophilic head groups.^{41–44} The marked heterogeneity of the nanoparticle assembly on the TGD film may reflect an uneven distribution of modifiers in the amine film. The conditions used for grafting TGD are expected to give a multilayer film⁴⁵ and this may have non-uniform composition across the surface.

The nanoparticle assemblies are strongly attached to cationic TGD and HA surfaces. For both films, nanoparticle counts were the same, and the morphology was unchanged, after 15 s ultrasonication in water; similar treatment in 1 M HCl had no detectable effect on a nanoparticle assembly on TGD. On the other hand, 15 s ultrasonication in 1 M NaOH led to aggregation of the nanoparticle assembly on a TGD surface. Under these conditions, the amine moieties of the surface film will be uncharged and hence the nanoparticle assembly is not stabilised by electrostatic interactions. This allows aggregation to be induced in the high ionic strength medium. (Aggregation also occurs in a nanoparticle solution which is adjusted to pH > 12 by the addition of concentrated NaOH solution.) The stability of nanoparticle assemblies on TGD to potential cycling was also briefly examined. Cyclic scans were obtained at 100 $mV s^{-1}$ in phosphate buffered

Table 1 Conditions for preparation of amine films and Au nanoparticle assemblies, and resultant nanoparticle densities obtained from SEM micrographs

	Film preparation		Assembly conditions			
	Amine	Electrolysis time (s)	Time (min)	pH	Solution concentration (nanoparticles L^{-1})	Nanoparticles assembled/ $10^4 nm^2$
1	TGD	600	180	4.2	1.3×10^{16}	36 ± 8 ($n = 3$) ^a
2	TGD	120	180	4.2	1.3×10^{16}	9 ± 5 ($n = 4$)
3	TGD	20 scans ^b	180	4.2	1.3×10^{16}	25 ± 3 ($n = 2$)
4	TGD	600	180	7	1.3×10^{16}	25 ± 6 ($n = 2$)
5	TGD	600	180	8	1.3×10^{16}	3 ± 3 ($n = 2$)
6	TGD	600	180	12	1.3×10^{16}	1 ± 1 ($n = 2$)
7	TGD	600	1	4.2	1.3×10^{16}	1 ± 2 ($n = 2$)
8	TGD	600	22	4.2	1.3×10^{16}	20 ± 4 ($n = 2$)
9	TGD	600	60	4.2	1.3×10^{16}	33 ± 5 ($n = 2$)
10	TGD	600	1560	4.2	1.3×10^{16}	35 ± 4 ($n = 2$)
11	TGD	600	180	4.2	6.5×10^{15}	22 ± 2 ($n = 1$)
12	TGD	600	180	4.2	1.3×10^{15}	2 ± 2 ($n = 2$)
13	TGD	600	180	4.2	1.3×10^{14}	2 ± 2 ($n = 1$)
14	HA	600	180	4.2	1.3×10^{16}	12 ± 3 ($n = 3$)
15	MP	600	180	4.2	1.3×10^{16}	2 ± 2 ($n = 3$)
16	None	600	180	4.2	1.3×10^{16}	2 ± 2 ($n = 2$)

^a Number of samples. ^b Film prepared using 20 cyclic scans between 0 and 1.2 V at 100 $mV s^{-1}$.

saline (pH 7.4) and 0.1 M $[\text{Bu}_4\text{N}]\text{BF}_4$ -acetonitrile solutions. For each medium, two scans were recorded between 1 and -1.5 V (vs. SCE in the aqueous solution and vs. a Ag wire in the non-aqueous medium) and SEM micrographs obtained before and after each electrochemical experiment showed no change in nanoparticle density or appearance of the assembly. The nanoparticle assemblies can also be stored in air for at least 12 months with no detectable changes.

Control of Au nanoparticle assembly at TGD surfaces

A useful characteristic of electrochemical grafting procedures is that the amount of modifier attached to the surface can be easily controlled through the choice of grafting conditions.²⁸ Concentration of the amine modifier, the grafting time and the potential applied during grafting all influence the amount of grafted film. This gives very simple methods for modulating the number of amine sites on the surface and hence the nanoparticle assembly. As an example of this approach, TGD was grafted to the PPF surface using the same solution conditions as in the standard procedure but applying only a 120 s electrolysis time. After 3 h immersion in the nanoparticle solution at pH 4.2 (Fig. 2E), the number of nanoparticles assembled on the surface $(9 \pm 5)/10^4 \text{ nm}^2$ is only 25% the number assembled on a film prepared with 600 s electrolysis time. This result clearly demonstrates that a lower surface concentration of cationic sites gives a lower nanoparticle density. When the TGD film was grafted using 20 cyclic scans at 100 mV s^{-1} between 0 and 1.2 V, the nanoparticle density was $(25 \pm 3)/10^4 \text{ nm}^2$.

Adjusting the pH of the nanoparticle solution is an alternative approach to controlling the number of cationic sites in the surface film. Liu and co-workers have demonstrated that the surface coverage of citrate-capped Au nanoparticles on *p*-aminothiophenol-modified Au surfaces depends on the pH of the Au nanoparticle solution and closely follows the expected extent of protonation of the aminothiophenol layer.¹⁰ Using the same approach for this work, Au nanoparticles were assembled on TGD films after adjusting the pH of the nanoparticle solution to 7, 8 and 12 (Table entries 4–6). The density of the nanoparticle assembly decreases as the pH increases; Fig. 2F shows the assembly prepared in pH 8 solution. The plot of nanoparticle density vs. pH in Fig. 3A suggests that there is a protonation constant close to 7.5 for the surface-attached film. This is within the expected range for the second protonation constant of a diamine, confirming that the nanoparticle density is controlled by the number of cationic sites in the surface film. Control of solution pH can thus be used to systematically vary the density of nanoparticle assemblies on these surfaces.

Other simple methods for controlling the nanoparticle assembly are to vary the immersion time of the grafted film in the nanoparticle solution (Table entries 7–10), and to adjust the concentration of the nanoparticle solution (Table entries 11–13). Fig. 3B shows that reducing the immersion time below 1 h reduces the density of the nanoparticle assembly. For a set immersion time of 3 h, the nanoparticle density is decreased as the particle concentration in solution is decreased (Fig. 3C).

Considering the range of strategies for varying nanoparticle assembly, controlling the number of cationic sites in the sur-

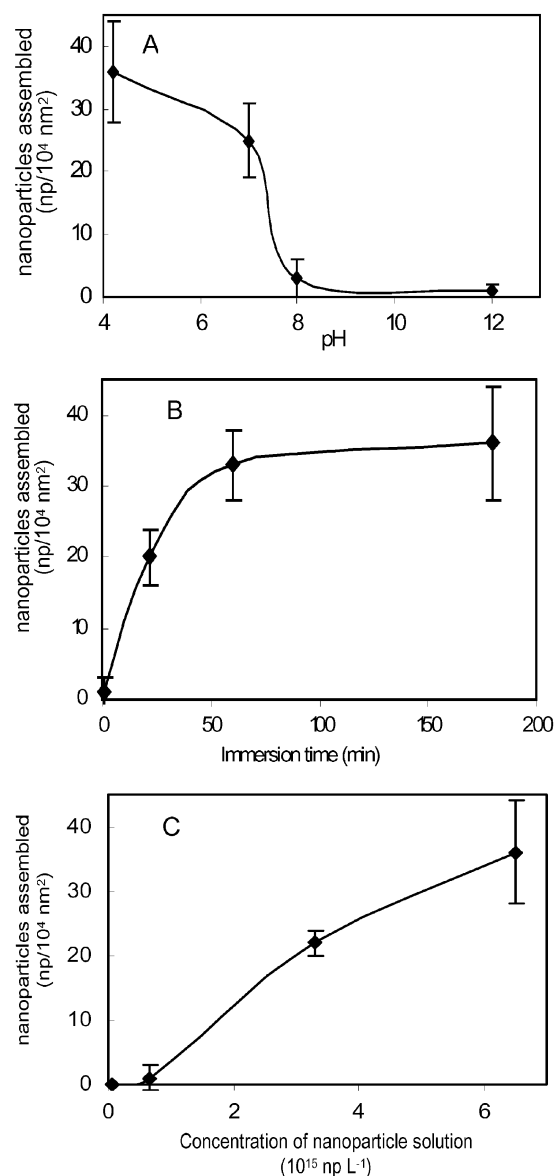


Fig. 3 Plots showing the effects of (A) nanoparticle solution pH, (B) immersion time and (C) concentration of nanoparticle solution on the density of nanoparticle assemblies on TGD films. TGD films were prepared using 600 s electrolysis time. (A), (B) nanoparticle concentration = 1.3×10^{16} ; (B), (C) solution pH is 4.2; (A), (C) immersion time = 180 min. Lines are provided as visual guides.

face film through choice of the grafting conditions is the most attractive approach. Adjusting the contact time between the surface and nanoparticle solution, and adjusting the concentration of the nanoparticle solution with fixed immersion time, have the disadvantage that the nanoparticle assembly has not reached its limiting density for the particular set of conditions. Small variations in time are expected to give significant variations in the nanoparticle density. On the other hand, adjusting the pH of the nanoparticle solution has the disadvantage that there is a large change in nanoparticle density with a relatively small change in pH between 7 and 8, which makes fine tuning of the assembly difficult. In contrast, generating variable numbers of amine sites directly through the grafting processes

enables nanoparticle assemblies of different limiting densities to be assembled under the chosen pH conditions. Formation of stable surface films with controlled densities of active sites can be difficult with other film attachment strategies such as self assembly of alkanethiols on Au, and silanes on silicon surfaces. However with electrochemical grafting it is a straightforward procedure.

Conclusion

Electrochemical grafting of amines to carbon surfaces is a simple and versatile approach to preparation of Au nanoparticle assemblies. The tether film is attached to the surface by a stable C–N bond and a wide range of commercially-available amines can be attached by this method. This gives opportunities for tuning the characteristics of the nanoparticle assembly, and other properties of the surface. The electrochemical grafting procedure is easily adjusted to give the desired surface concentration of cationic sites and thus density of electrostatically assembled nanoparticles. Control of assembly conditions can also be used for tuning the nanoparticle assembly. In addition to the ease of preparation and stability of these tethered nanoparticle assemblies, the use of carbon as the substrate is attractive for applications such as low cost, high surface area catalytic materials and low cost disposable electrochemical sensors. In ongoing work we are investigating the catalytic properties of size- and density-selected tethered Au nanoparticles on carbon substrates.

Acknowledgements

This work was supported by the University of Canterbury and the MacDiarmid Institute for Advanced Materials and Nanotechnology. Emelyn Tan thanks the MacDiarmid Institute, and Samuel Yu thanks the Tertiary Education Commission, for doctoral scholarships. We thank Mr Manfred Ingerfeld for carrying out TEM measurements.

References

- For recent reviews see: (a) M. Brust and C. J. Kiely, *Colloids Surf., A*, 2002, **202**, 175; (b) M.-C. Daniel and D. Astruc, *Chem. Rev.*, 2004, **104**, 293.
- K. C. Grabar, R. G. Freeman, M. B. Hommer and M. J. Natan, *Anal. Chem.*, 1995, **67**, 735.
- S. Liu, R. Maoz and J. Sagiv, *Nano Lett.*, 2004, **4**, 845.
- L. Maya, K. A. Stevenson, G. Muralidharan, T. G. Thundat and E. A. Kenik, *Langmuir*, 2002, **18**, 2392.
- P. M. Mendes, S. Jacke, K. Critchley, J. Plaza, Y. Chen, K. Nikitin, R. E. Palmer, J. A. Preece, S. D. Evans and D. Fitzmaurice, *Langmuir*, 2004, **20**, 3766.
- J. Wang, T. Zhu, J. Song and Z. Liu, *Thin Solid Films*, 1998, **327–329**, 591.
- O. Seitz, M. M. Chehimi, E. Cabet-Deliry, S. Truong, N. Felidj, C. Perruchot, S. J. Greaves and J. F. Watts, *Colloids Surf., A*, 2003, **218**, 225.
- S. Liu, T. Zhu, R. Hu and Z. Liu, *Phys. Chem. Chem. Phys.*, 2002, **4**, 6059.
- J. Tien, A. Terfort and G. M. Whitesides, *Langmuir*, 1997, **13**, 5349.
- T. Zhu, X. Fu, T. Mu, J. Wang and Z. Liu, *Langmuir*, 1999, **15**, 5197.
- L. M. Demers, S.-J. Park, T. A. Taton, Z. Li and C. A. Mirkin, *Angew. Chem., Int. Ed.*, 2001, **40**, 3071.
- L. M. Demers, D. S. Ginger, S. J. Park, Z. Li, S. W. Chung and C. A. Mirkin, *Science*, 2002, **296**, 1836.
- H. Zhang, Z. Li and C. A. Mirkin, *Adv. Mater.*, 2002, **14**, 1472.
- Y. Yamanoi, T. Yonezawa, N. Shirahata and H. Nishihara, *Langmuir*, 2004, **20**, 1054.
- E. W. L. Chan and L. Yu, *Langmuir*, 2002, **18**, 311.
- X. Huang, H. Huang, N. Wu, R. Hu, T. Zhu and Z. Liu, *Surf. Sci.*, 2000, **459**, 183.
- K. C. Grabar, P. C. Smith, M. D. Musick, J. A. Davis, D. G. Walter, M. A. Jackson, A. P. Guthrie and M. J. Natan, *J. Am. Chem. Soc.*, 1996, **118**, 1148.
- D. J. Tognarelli, R. B. Miller, R. R. Pompano, A. F. Loftus, D. J. Sheibley and M. C. Leopold, *Langmuir*, 2005, **21**, 11119.
- A. J. Downard, *Electroanalysis*, 2000, **12**, 1085.
- B. Barbier, J. Pinson, G. Desarmot and M. Sanchez, *J. Electrochem. Soc.*, 1990, **137**, 1757.
- R. S. Deinhammer, M. Ho, J. W. Anderegg and M. D. Porter, *Langmuir*, 1994, **10**, 1306.
- J. A. Harnisch, A. D. Pris and M. D. Porter, *J. Am. Chem. Soc.*, 2001, **123**, 5829.
- R. Zanella, E. V. Basiuk, P. Santiago, V. A. Basiuk, E. Mireles, I. Puente-Lee and J. M. Saniger, *J. Phys. Chem. B*, 2005, **109**, 16290.
- K. H. Saunders and R. L. M. Allen, *Aromatic Diazo Compounds*, Edward Arnold, London, 1985.
- P. A. Brooksby and A. J. Downard, *Langmuir*, 2004, **20**, 5038.
- A. Adenier, M. M. Chehimi, I. Gallardo, J. Pinson and N. Vila, *Langmuir*, 2004, **20**, 8243.
- K. J. Hoekstra and T. Bein, *Chem. Mater.*, 1996, **8**, 1865.
- A. J. Downard and A. Bin Mohamed, *Electroanalysis*, 1999, **11**, 418.
- J. Liu and S. Dong, *Electrochem. Commun.*, 2000, **2**, 707.
- X. Han, L. Wang, B. Qi, X. Yang and E. Wang, *Anal. Chem.*, 2003, **75**, 6566.
- H. Tanaka and A. Aramata, *J. Electroanal. Chem.*, 1997, **437**, 29.
- E. Coulon, J. Pinson, J.-D. Bourzat, A. Commercon and J. P. Pulicani, *Langmuir*, 2001, **17**, 7102.
- E. Coulon, J. Pinson, J.-D. Bourzat, A. Commercon and J.-P. Pulicani, *J. Org. Chem.*, 2002, **67**, 8513.
- F. Geneste and C. Moinet, *New J. Chem.*, 2005, **29**, 269.
- S. Antoniadou, A. D. Jannakoudakis, P. D. Jannakoudakis and E. Theodoridou, *J. Appl. Electrochem.*, 1992, **22**, 1060.
- D. A. Buttry, J. C. M. Peng, J.-B. Donnet and S. Rebouillat, *Carbon*, 1999, **37**, 1929.
- M. A. Hayes and W. G. Kuhr, *Anal. Chem.*, 1999, **71**, 1720.
- R. Kostecki, B. Schnyder, D. Allia, X. Song, K. Kinoshita and R. Kotz, *Thin Solid Films*, 2001, **396**, 36.
- S. Ranganathan and R. L. McCreery, *Anal. Chem.*, 2001, **73**, 893.
- P. A. Brooksby, A. J. Downard and S. S. C. Yu, *Langmuir*, 2005, **21**, 11304.
- K. Slowinski, R. V. Chamberlain, C. J. Miller and M. Majda, *J. Am. Chem. Soc.*, 1997, **119**, 11910.
- K. Slowinski, K. U. Slowinska and M. Majda, *J. Phys. Chem. B*, 1999, **103**, 8544.
- A. M. Becka and C. J. Miller, *J. Phys. Chem.*, 1993, **97**, 6233.
- M. French and S. E. Creager, *Langmuir*, 1998, **14**, 2129.
- A. J. Downard, S. L. Jackson and E. S. Q. Tan, *Aust. J. Chem.*, 2005, **58**, 275.